SPECIFIC SMALL-SCALE VORTICES ("VORTEX COLUMNS") IN THE SEA SHELF AREAS DUE TO THE NEAR-BOTTOM CONVECTION

V.G.Bondur[1], Yu.V.Grebenyuk[1], R.N. Keeler[3], K.D.Sabinin[1] , S.I.Muyakshin[2], C.H. Gibson[4]

[1] AEROCOSMOS Research Institute for Aerospace Monitoring, Moscow, Russia

[2] Lobachevsky State University of Nizhni Novgorod

[3] Directed Technology, Inc., Arlington, VA, USA,

[4] University of California San Diego, La Jolla, CA, USA

[1] vgbondur@aerocosmos.info

[1] grebenyk@gmail.com

[1] ksabinin@yandex.ru

[2] serg_mun@list.ru

[3] rnkeeler@verizon.net

[4] cgibson@ucsd.edu

ABSTRACT

Complex interactions of turbulence, fossil turbulence and fossil turbulence internal waves in the stratified coastal ocean are studied at municipal outfall locations in Hawaii (Honolulu, USA) and the Black sea (Gelendzhik, Russia) using acoustic Doppler profiling. A near-vertical, stratified turbulent mixing process* produces intermittent, concentrated vortex columns identified as generic by microstructure measurements near the outfall in Honolulu and Gelendzhik. The columns extract energy from near bottom mean flows, and serve as mixing channels for the stratified turbulence vortices and internal wave systems. Persistent patterns of sea surface disturbances produced by submerged turbulence, fossil turbulence, and radiated fossil turbulence internal waves of the outfall are subject to remote sensing by space satellites, as well as by acoustic Doppler profiling.

INTRODUCTION

* Beamed Zombie Turbulence Maser Action (BZTMA) mixing chimneys

Experimental research in the sea shelf areas near Honolulu (Oahu Island, Hawaii, USA) [Bondur, 2006, 2011; Keeler et al., 2005; Gibson et al., 2006ab] have allowed us to reveal very specific peculiarities of current fields sporadically appearing in the water column. These peculiarities look like very sharp change of current velocity with simultaneous turn of the current vector [Bondur et al., 2009a, 2009c, 2011]. Such specific features of currents are due to thin (compact) vortices ("vortex columns") passing through acoustic profiler (ADCP) beams. These peculiarities are originated from intensive discharges of almost non-salty water through submerged collectors. Convective plumes of low-salinity water come to the surface in form of compact vortices. Discharged non-salty wastewater trapped by such vortices may travel at relatively long distances [Bondur, 2006, 2011; Bondur et al., 2009c]. The vortex columns of these studies may be identified with the (BZTMA) mixing chimneys [Keeler et al., 2005; Gibson et al., 2006ab] observed in Hawaii. Thousands of hydrodynamic phase diagrams were collected. Fossil turbulence wave radiation attributed to advected outfall fossil turbulence patches was detected to distances up to 40 km. GPS equipped parachute drogues were released at the outfall to confirm the advection directions [Bondur, 2006, 2011; Leung, 2011].

Below are the results of detailed experimental research of these phenomena carried out in the coastal water area in the Mamala Bay (Honolulu, Oahu Island, USA) and near Gelendzhik (Black Sea, Russia).

Mathematical modelling of ADCP response to passing column-like vortices with diameters less than the depth has proved this hypothesis.

STUDY OF SMALL-SCALE VORTICES IN THE MAMALA BAY WATER AREA (HAWAII, USA)

Within 2002 and 2005 there had been performed comprehensive studies on the Hawaiian shelf in the Mamala Bay water area (Oahu Island, USA) of anthropogenic impacts on the coastal water area ecosystems due to deep wastewater discharges [Bondur, 2006, 2011; Keeler et al., 2005; Bondur, Tsidilina, 2006; Bondur et al., 2007; Gibson et al, 2006ab, 2007ab]. For a long

time during those experiments characteristics of currents, sound scattering layers and temperature had been measured using moored thermistor chains and bottom-mounted three-beam acoustic Doppler current profilers (SonTek ADP 250 kHz) [Bondur, Tsidilina, 2006; Keeler et al, 2004; Bondur et al., 2007]. Besides, satellite imaging using optical and radar instruments aboard various satellites had been performed, allowing us to study surface manifestations of deep wastewater discharges. The results of those studies were summarized in [Bondur, 2011].

Fig. 1 shows stations for measurements of temperature vertical profiles (AT, BT, and CT stations) and three current vector components (Av, Bv, and Cv stations), as well as the collector with the diffuser for wastewater discharge into Mamala Bay waters.

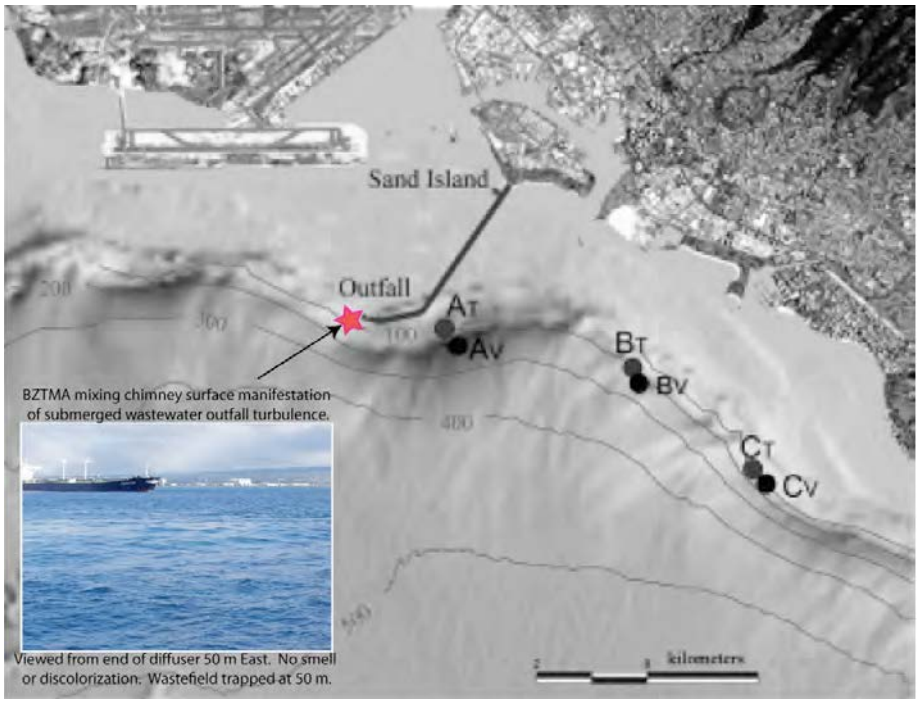

Fig. 1. The schematic for temperature and current velocity measurement stations in Mamala Bay. Insert shows surface manifestations of outfall turbulence trapped at 50 m about 50 m west of the end of the outfall diffuser pipe. Such observable surface smoothing manifestations of the outfall are rare, with little or no discoloration of surface waters and no smell, suggesting their BZTMA (beamed zombie turbulence maser action) mixing chimney origin.

Current field characteristics were measured at the depths between 4 and 76 m each 2 meters and every 1 minute. Water temperature was measured every 0.5 – 2 min [Bondur, Tsidilina, 2006; Bondur et al., 2007, 2009b].

The analysis of current characteristics have revealed large surges of current velocities. The probability of such surge appearance significantly exceeds the values typical for the Gaussian process [Bondur et al., 2009a, 2009c; 2011]. Extreme surges of current velocities were revealed at all the stations for the whole period of measurements in the Mamala Bay water area in initial current values as well as in their high-frequency components (more 1 cycle/hour). Amplitude of horizontal current velocity surges reached ± 30 cm/s with ~ 4 cm/s mean square error, and their duration did not exceed 2-3 min. Both unipolar surges (positive or negative pulses) and bipolar ones (when the pulse polarity change was every 1 min) were observed. Bipolar pulse current jumps were observed more rarely than unipolar, though they were most interesting. Depth smoothing of measurements was applied to decrease errors (smoothing by 10 m).

Frequency of current velocity pulse surge observations in the water area of interest can be judged by current analysis results obtained in the course of 19 days at the Bv Station in 2004. At that station at depths of 12-70 m 920 pulses were registered whose amplitudes exceeded mean square error of measurements no less than by 3.5-fold.

The examples of typical bipolar pulse surges of current velocities registered at observation stations in the Hawaiian shelf area are given in Figs. 2, a,b,c. The analysis of given figures shows that weak chaotic high-frequency currents suddenly changed by sharply strengthening currents equally directed almost in the whole water column. And current directions after a minute unevenly changed to the opposite ones.

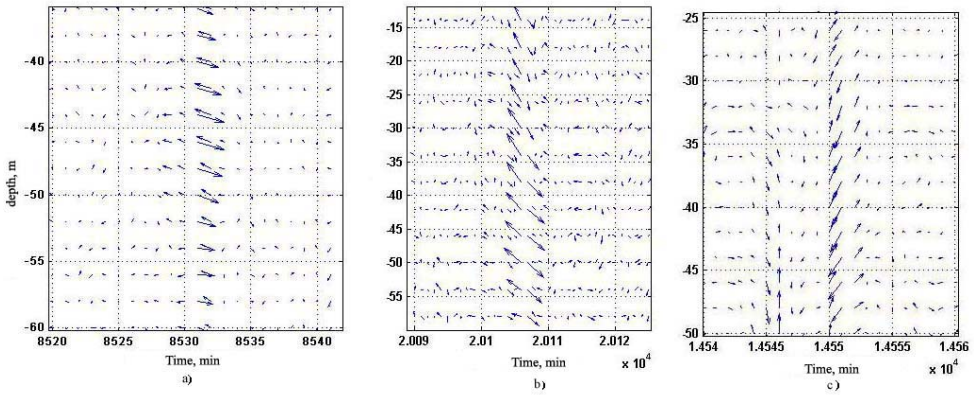

Fig. 2,a,b,c. Examples of bipolar pulse surges of high-frequency components of current velocities at Av (a), Bv (b), and Cv (c) stations. The arrows denote the current vectors (north is up). X, Y-axis show the observation time (min) at the station and depth levels.

To find out grounds of such strong surges of current velocities, first of all it was checked whether they had been caused by internal wave solitons. For this purpose, the comprehensive analysis of characteristics in solitons and bipolar current surges was performed using every minute current and temperature profiles. The feature of solitons is that as opposed to current surges of interest the extrema of vertical velocities are observed on both sides of horizontal velocity maximum [Konyaev, Sabinin, 1992]. It was established that as opposed to solitons, the moments of horizontal velocity surges coincided with the moments of vertical velocity extrema (see Fig. 2).

Since the surges of current velocity registered by ADCP could be related to movements of organisms scattering sound (zooplankton, fish shoals), during the analysis the special attention was paid to the absence of high echo intensity registered by all three ADCP beams. Simultaneous error surges at many horizons is unlikely too.

To explain the reasons of current velocity surges detected in the Mamala Bay water area, a hypothesis was suggested that specific manifestations of small-scale current variability registered by ADCP on the shelf in the area of deep wastewater discharge had been related to thin vortices (“vortex columns”) appearing during outflow and rise of non-salty wastewater from the diffuser [Bondur et al, 2009a, 2009c, 2011].

Surfacing of discharged wastewaters near the diffuser was repeatedly registered during hydrophysical measurements in the Mamala Bay water area (Fig. 3) [Bondur, 2011]. Fig. 3, b,d shows the example of a surface anomaly due to such water surfacing. Photos were taken form the research ship. The anomalous plumes are discerned on the sea surface by colour and wave structure. Surfacing of the plume at the same time was also registered using submersible AC-9 hydrooptical instrument (Fig. 3, a). Fig. 3, c shows the diagram of 2D distribution of large

particle concentration using AC-9 data on August 12, 2004 (08:00 LT) [Bondur, 2011]. Fig. 3, a, c shows model estimates of the float-up depth of wastewater jets during these periods [Bondur, 2011].

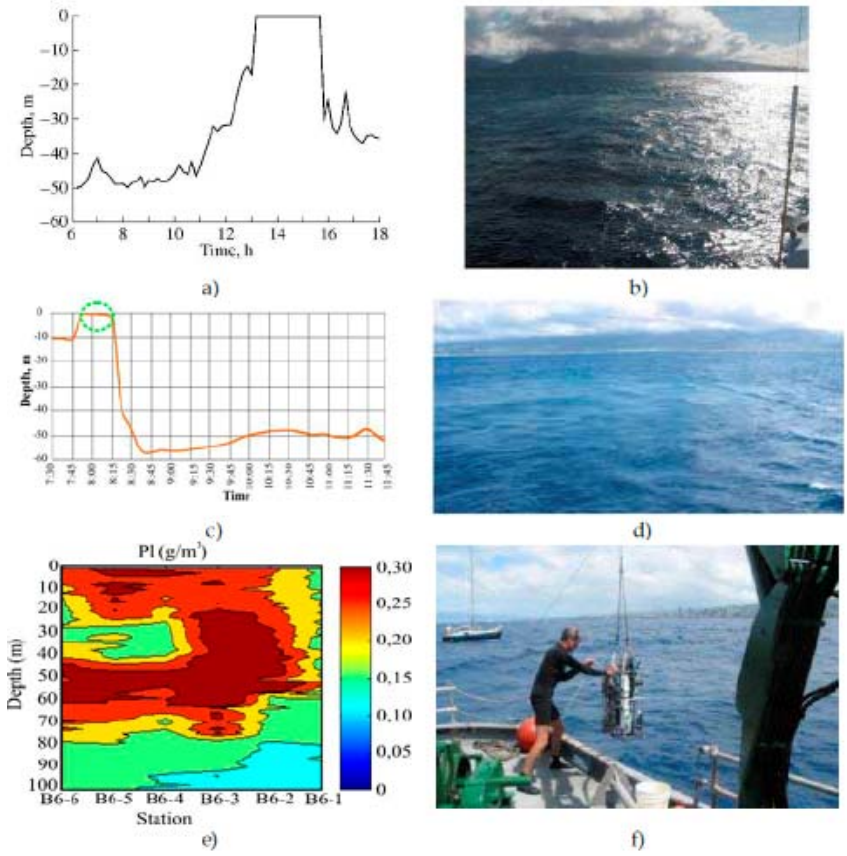

Fig. 3. Comparison of the model estimates of the parameters of the jet with the data of experimental measurements: (a) and (c) Model estimates of the float-up depth of the sewage jet in the period from 6:00 to 18:00 on September 6, 2002 (a) and from 07:30 to 11:45 on August 12, 2004 (c); (b) and (d) Photos of the surface anomaly caused by the deep-water discharge measured from a ship near the diffuser on September 6, 2002, (b) and at 08:00 on August 12, 2004 (d); 2D profile of large particle concentration obtained by AC-9 (e); AC-9 deployment (f).

MODELLING 3-BEAM ADCP RESPONSE TO VORTEX STRUCTURE PASSING THROUGH IN THE MAMALA BAY WATER AREA

To confirm the hypothesis that pulse surges of current velocities are due to passing of such "vortex columns" through ADCP beams, mathematical modelling of the Doppler Profiler response to a thin vertical vortex passing by using spatial scale considerably less than the distance between its beams [Bondur et al, 2009, a]. By ADCP response we understand time

realization of three values which in the case of uniform field of current velocity would be its V_X, V_Y, and V_Z projections on the rectangular coordinate system related with the instrument.

To obtain velocity in three dimensions by using ADCP, one must assume that currents are uniform (homogeneous) across layers of constant depth. Thus, it is possible to correctly measure velocities using ADCP only if the scale of current inhomogeneities is considerably larger than the distance between ADCP beams [ADCP Coordinate…, 2008]. Minute velocity jumps in ADCP data can not be related with quite large spatial scales and so they only indicate inhomogeneities of current field between the measuring instrument beams. Therefore, strictly speaking, it is not possible to obtain the correct picture of currents in such a fine inhomogeneity as a vortex column (a vortex whose height is larger than its diameter) using ADCP.

For 3-beam instrument, V_X, V_Y, V_Z current velocity projections can be calculated using the following matrix transformation

$$\begin{pmatrix} \frac{-2}{3\sin\Theta} & \frac{1}{3\sin\Theta} & \frac{1}{3\sin\Theta} \\ 0 & \frac{-1}{\sqrt{3}\sin\Theta} & \frac{1}{\sqrt{3}\sin\Theta} \\ \frac{1}{3\cos\Theta} & \frac{1}{3\cos\Theta} & \frac{1}{3\cos\Theta} \end{pmatrix} \begin{pmatrix} V1 \\ V2 \\ V3 \end{pmatrix} = \begin{pmatrix} Vx \\ Vy \\ Vz \end{pmatrix} \qquad (1)$$

Here V_i, i=1,2,3 are the projections of current velocity on ADP beam axes; Θ - angle of beam axes vertical deviation, Θ=25°.

To model the dependence of instrument output values on time, we need to compute how projections of currents on the ADCP beams change depending on various positions of a vortex in relation to the instrument. The Rankin vortex was taken as a vortex model. It is a cylindrical vortex having a vertical axis and solid rotation in the interior (R_0 radius) where the velocity increases linearly as moving off the centre to V_{max} maximum value, and than it decreases inversely proportional to the distance under $V=V(R_0)R_0/R$ law [Bondur et al., 2011]. To model the ADCP response to vortex passing, the computation scheme have been developed for fluid

velocity projections on the instrument beams depending on the vortex distance to the instrument centre and distance elements.

Strictly speaking, vortex passing modelling should allow for velocity of homogeneous current which transfers the vortex. However, since the experimental velocity realizations were subjected to high-frequency filtering, we may not to allow for the transfer velocity and actually calculate only its deviations. To model ADCP response to vortex passing, a calculation scheme was developed for V_i fluid velocity projections on the instrument beams depending on the distances between vortex and instrument centre and distance elements. The instrument centre position (a point from which projections of its beams on the horizontal plane go) was given by X, Y coordinated relative to the vortex axis. D is the beam projection length. This value depends on the Z_0 height above the bottom where velocity measurement was carried out: $D=tg(\Theta)Z_0$. The distance between the vortex centre and the instrument centre is r_0, and r_i (i=1,2,3) are the distances from the vortex centre to the relevant distance elements. Then the following expressions can be obtained for current velocity projections on the beams:

$$V_i = V(r_i)\cdot\sin(\arccos(\frac{D^2+(r_i^2-r_0^2)}{2Dr_i}))\cdot\sin(\Theta)\ , \qquad (2)$$

where r_0, r_i , V(r) values can be calculated using the following formulae:

$$r_0 = \sqrt{X^2+Y^2} \qquad (3)$$

$$r_1 = \sqrt{X^2+(D+Y)^2} \qquad (4)$$

$$r_2 = \sqrt{(X-D\sin(\pi/3))^2+(Y-D\cos(\pi/3))^2} \qquad (5)$$

$$r_3 = \sqrt{(X+D\sin(\pi/3))^2+(Y-D\cos(\pi/3))^2} \qquad (6)$$

$$V(r) = \begin{cases} V_{\max}\dfrac{r}{R_0} & where\ \ r \le R_0 \\ V_{\max}\dfrac{R_0}{r} & where\ \ r \ge R_0 \end{cases} \qquad (7)$$

The special code was developed for these calculations by which the response to a vortex passing over the instrument was modelled.

The ADCP response to vortex passing depends on many parameters, including R_0 and V_{max}, sense of vortex rotation, velocity and direction of its moving, location of vortex trajectory in relation to the instrument, vortex beam orientation, measurement resolution, and even on the fact in which moments of the vortex passing over the ADCP the measurements were carried out (if the measurements were not very frequent, a narrow vortex might not be reflected in the measurements quite detailed). The calculations of current velocities were carried out for a wide range of vortex parameter values. These calculations have shown that passing of narrow vortices though ADCP beams caused sharp surges in current velocities measured by the instrument. Amplitude of surges and their kind (unipolar, bipolar) depend on vortex position in relation to ADCP and direction of its movement [Bondur et al., 2011].

Fig. 4 shows an example of model calculation comparison (Fig. 4, b) with the data of in-situ measurements of current velocities (Fig. 4, a) obtained at Bv point in 2004 between 20095-20115 minutes of measurements. Among many studied options the one case most of all fits to the picture observed in this point, when the anticyclone vortex with the parameters R_0=5 m and V_{max}=0.4 m/s) moves east-southeast. Note, that for other options of model vortex passing, the ADCP response could change significantly, taking the form of a single peak and less significant vector rotation in double pulse, but in most cases such a turn took place in 1-2 minutes.

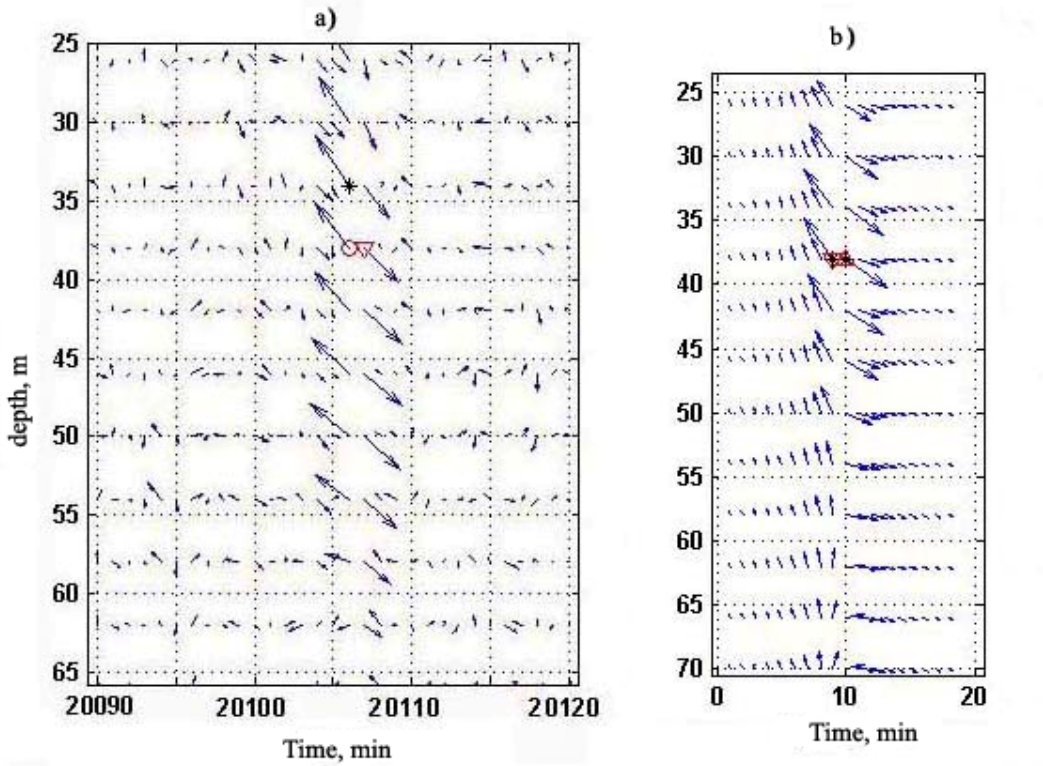

Fig. 4. a – pulse surge of high-frequency (more than 10 cycle/hour) currents registered at 20106th minute of measurement at Bv point (an asterisk denotes the horizontal velocity maximum, circle and triangles denote vertical velocity extrema); b – current vector using the ADCP response to anticyclone Rankine vortex with 5 m radius and 0.4 m/s maximum velocity which passes by ADCP to the south-east with 0.2 m/s velocity.

The analysis of Fig. 4 demonstrates satisfactory correlation of model calculations and in-situ data, what confirms the suggested hypothesis.

EXPERIMENTAL STUDIES OF SMALL-SCALE VORTICES IN GELENDZHIK SHELVE AREA IN THE BLACK SEA

To confirm the hypothesis about the mechanism of strong surges of current velocities which was suggested based on the results from the research in the Hawaiian shelf area in 2009 – 2011 there had been carried out studies of current fields in Gelendzhik shelf area of the Black Sea (Russia) near the deep wastewater discharge. In the case of the Gelendzhik shelf as for the Hawaiian shelf area wastewaters are discharged through the submerged collector. Low-salinity

wastewater surfaces in the form of a plume, because it is lighter then surrounding salty waters. In such a convective plume we can expect vortex structures similar to Hawaiian ones.

The map of the studied region is given in Fig. 5. As opposed to the experiments in the Mamala Bay, current velocity measurements were carried out using 4-beam bottom ADCP (Rio Grande 600 kHz). Fig. 5 shows the collector for submerged wastewater discharge. Current velocity measurements in the Gelendzhik shelf area were performed using the bottom-mounted ADCP which was installed near the end of the collector at a depth of 31.5 m. The location of the bottom profiler is denoted with an asterisk in Fig. 5. The experiments carried out in 2009-2011 were every 1 min and every 0.5 m. Below are the results from measurement data processing and analysis in 2009.

The analysis of these experimental data have revealed large surges of current velocities similar to those observed on the Hawaiian shelf in the Mamala Bay [Bondur et al., 2009a, 2009c, 2011]. To decrease errors, depth smoothing was applied (over 4 meters). The analysis of surges in high-frequency current velocity components have shown that the amplitude of horizontal velocity surges reached ± 15 cm/s (~ 1.72 cm/s mean-root error), and their duration did not exceed 2 – 3 min. As on the Hawaiian shelf, both unipolar and bipolar surges were observed, while current directions reversed in 1 – 2 min.

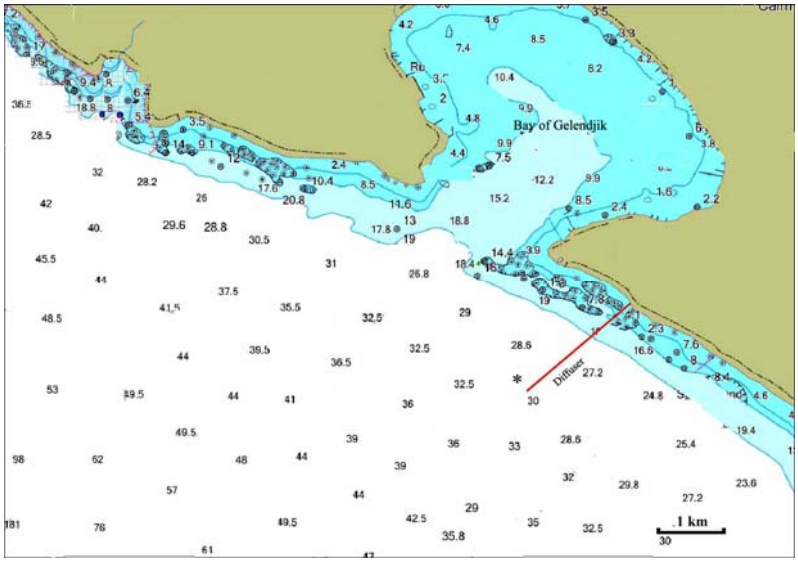

Fig. 5. Map of hydrophysical measurements in the Black Sea shelf area.

During the analysis of surges, the attention was paid to the fact that all ADCP beams had not detected sound scattering surges caused by motions of organisms scattering sound. During the process of measurements significant change of the background current direction and velocity took part at the location of the bottom profiler. For example, on October 6 – 8, 2009 (counts from 1 to 3300 min) depth-averaged background currents had northwestern direction with 10-20 cm/s velocity, which reversed further to southeastern (Fig. 6). The observed change in current directions was caused by passage of a large vortex which was often observed in the coastal area of the Black Sea [Zatsepin et al, 2010].

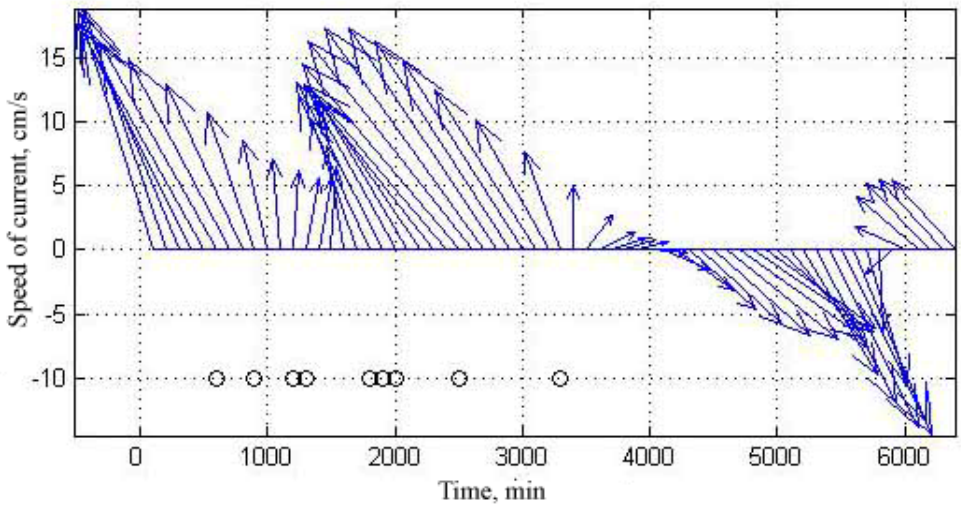

Fig. 6. Vectors (north is up) of barotropic (depth-averaged) low-frequency currents based on bottom ADCP data (October 6 – 10, 2009). Circles denote the moments of well-expressed bipolar pulses.

The analysis of large and sharp surges of current velocities occurred simultaneously at various depths have shown that they were observed only in the period when currents had had northwest direction. This result is completely explainable in terms of the suggested mechanism of surges in the area of coastal convection.

As one can see in Fig. 5, the bottom ADCP was installed at the short haul to the northwest from the wastewater collector outlet. Under the influence of northwest currents surfacing wastewater plumes were transported to the profiler where under the influence of developing convection vortices had been occurring which caused surges in ADCP data. After current

direction reversing to southwestern, the convective plume was not transported to the ADCP and vortices were not registered.

The examples of extremely large bipolar surges of current velocities in Gelendzhik shelf area are given in Figs. 7 a-c. These surges occurred against weak chaotic high-frequency fluctuations when currents sharply strengthened almost over the whole water column and their directions reversed very rapidly after 1 – 2 minutes.

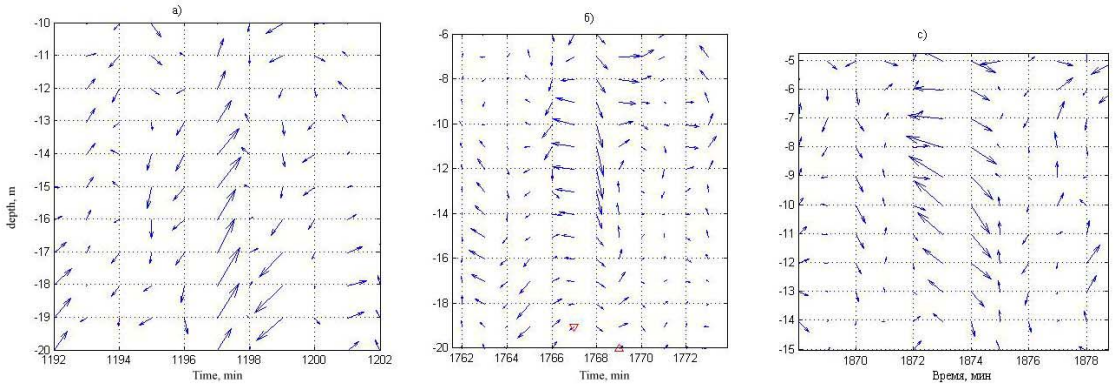

Fig. 7 a,b,c. The examples of strong bipolar pulse surges of high-frequency components of current velocities (more than 1 cycle/hour) at a) t=1192-1202 min; b) t=1760-1774 min; c) t=1868-1878 min.

The joint analysis of current characteristics, echo intensity, and vertical profiles of seawater temperature and density have allowed us to establish that the observed surges of current velocities were not caused neither by sound scattering objects nor internal waves which could not exist at that time because of almost complete uniformity of the whole water column above the ADCP.

Using 4-beam profiler we determined not only current velocities but their measurement errors. “Errors” are characterized by the “Error” instrument’s reading. This value is the difference between vertical velocity estimations for two pairs of instrument’s beams [ADCP Coordinate…, 2008]. Analysis of “Error” values allows us to determine time moments when current measurements were carried out with large inaccuracy. Fig. 8 a-c present diagrams of current vectors for 3 moments of surge observations (Fig. 7 a-c) and ADCP measurement error

values for these moments. In these figures, vectors are shown with arrows, and measurement errors are shown in greyscale.

The analysis of Figures 8 a-c have shown that maximum values of measurement errors correspond to the moments of large surges of current velocities. This is the evidence of the fact that the observed high current velocities were due to current field inhomogeneity within ADCP measurement range. Passing of small vortex through the ADCP beam causes current velocity surges in profiler data.

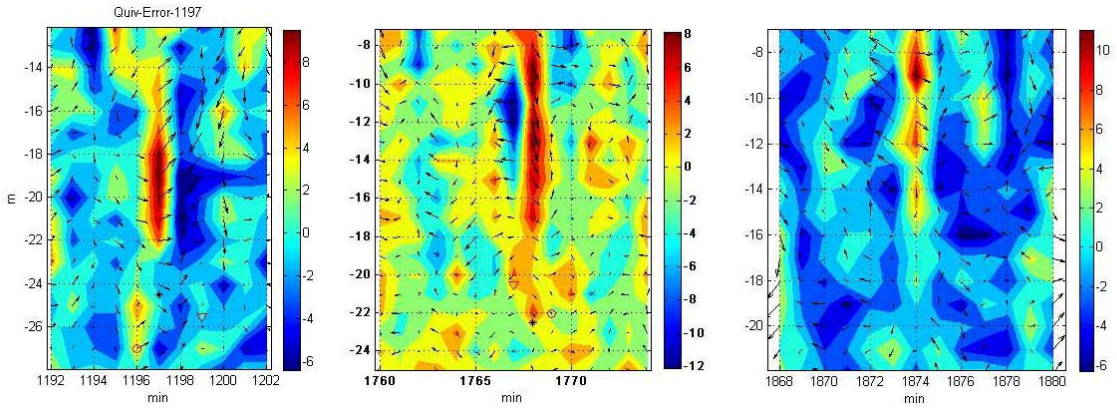

Fig. 8 a, b, c. Diagrams of current velocity vectors (arrows) and "error" values of velocity measurements (shade of grey) for three moments of observing large velocity surges: a - 1192-1202 min, b - 1760- 1774 min, c - 1868- 1880 min.

Note, that observation frequency of "vortex columns" in the Gelendzhik shelf area was lower than in the Hawaiian shelf area. It could be related with the lesser volume of discharged wastewater. Moreover, the discharged waters ran out not only from the collector outlet, but from some cracks in rusty tube. It was clear from the measurements of echo intensity carried out using towed ADCP. These measurements allowed one to detect draining of polluted wastewater from the cracks in the collector.

MODELING THE RESPONSE OF 4-BEAM ADCP TO VORTEX STRUCTURE PASSING IN THE GELENDZHIK SHELF AREA

In the Gelendzhik shelf area similar to Hawaiian shelf area studies there has been performed mathematical modelling of thin vortex passing through beams of an acoustic profiler. Four-beam ADCP was modelled as opposed to three-beam ADCP used in the experiments in Mamala Bay (Hawaii). As before, Rankine vortex was taken as a model vortex. For calculations, 4 – 10 m vortex radii were taken, what was considerably lesser than the distance between the beams of the instrument. Since the vortices of interest were related with convective motions in surfacing plumes of low-salinity wastewater, so it is natural to think that in the central part of a vortex upward streams prevailed, turning into downward on its periphery. For calculations, in the vortex there was given change of vertical currents from +2 cm/s in the central part of the vortex to -1 cm/s on its periphery.

V_X, V_Y, and V_Z current velocity projections and V_{err} measurement error were computed using the following matrix transformation:

$$\begin{pmatrix} Vx \\ Vy \\ Vz \\ V_{err} \end{pmatrix} = \begin{pmatrix} 1/2\sin\theta & -1/2\sin\theta & 0 & 0 \\ 0 & 0 & -1/2\sin\theta & 1/2\sin\theta \\ 1/4\cos\theta & 1/4\cos\theta & 1/4\cos\theta & 1/4\cos\theta \\ 1/2\sqrt{2}\sin\theta & 1/2\sqrt{2}\sin\theta & -1/2\sqrt{2}\sin\theta & -1/2\sqrt{2}\sin\theta \end{pmatrix} \begin{pmatrix} V_1 \\ V_2 \\ V_3 \\ V_4 \end{pmatrix} \qquad (8)$$

Here V_i, i=1,2,3,4 are the projections of current velocity on ADCP beam axes; Θ - angle of beam axes vertical deviation.

Calculations of current velocities were performed for a wide range of values of vortex parameters. These calculations have shown that passing of narrow vortices through ADCP beams leaded to sharp surges in current velocities. The amplitude of surges and their type (unipolar, bipolar) depended, first of all, on the position of a vortex relative to ADCP, velocity and direction of its movement.

Figs. 9 a,b give an example of the comparison of model calculations of current velocity values and measurement errors (Fig. 9 a) with in-situ data obtained on October 7, 2009 at 1192-1202 min of measurements (Fig. 9 b). In this Figure, current vectors are denoted with arrows,

and measurement "errors" are colour coded (shade of grey). The best agreement of model estimations with observation data for high-frequency currents was for the conditions when anticyclonic vortex having 8 m radius had been moving northwest 0.15 m/s velocity. Such vortex movement differs from passive transport by background current (0.07 m/s, northern direction).

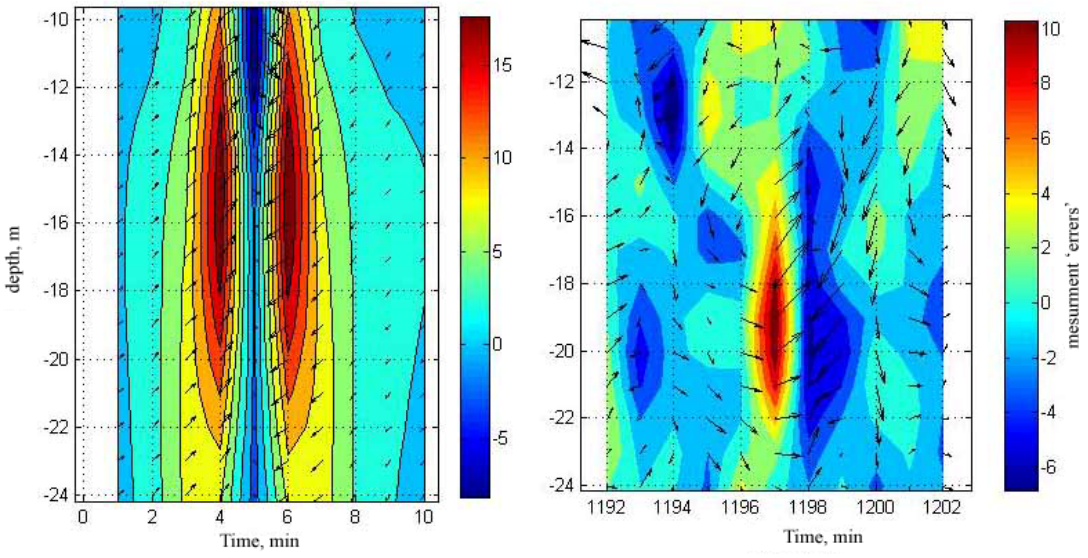

Fig. 9 a,b. Comparison of model calculation results and in-situ data by current vectors (arrows) and measurement "errors" (halftone code): a) ADCP model response to an anticyclonic vortex with 8 m radius moving northwest with 0.15 m/s velocity; b) current in-situ data at 1194-1202 min of observations.

Note, that an actual vortex can not completely fit the simplified model, especially, the shape of convective plumes in which vortices are generated can differ from vertical cylinder [Wood et al, 1993]. So even correlation of a pattern of vectors reversing in 2 minutes if "error" values turn from positive into negative in 1 minute in the model and in observations, allows us to believe that a compact anticyclonic vortex with the parameters mentioned above passed over the ADCP.

One noticeable difference of the model picture from the real one is a larger vertical length scale of the area where bipolar pulses are revealed than in observation, and manifestation of significant currents which are absent in the observations. Since real vortices are bent by background currents and have the shape of bent vortex cords similar to waterspouts rather than to

column-like vortices, such difference between the results of model calculations and observations is to be expected.

Apparently, that other observed pulses are related with thin "vortex columns" and their absence in the second half period of measurements quite agrees with the change of background current direction from north-western to south-eastern.

DISCUSSION

A new method has been developed based on acoustic Doppler profilers to detect concentrated vortices. Applications to outfall flows in Hawaii shelf and in Gelendzhik shelf areas show similar results. This is to be expected from a narrow definition of turbulence[†] based on the inertial vortex force [Gibson, 1986]. Turbulence in natural fluids is always identical at the smallest scales following the three Kolmogorov universal similarity laws, which are given a physical basis by this definition. Vortex dynamics of the inertial vortex forces describe the cascade of turbulent energy from the Kolmogorov scale to some larger scale where the energy is fossilized [Leung, 2011]. Detailed sea truth of the process was obtained in the Hawaii experiments [Keeler et al., 2005; Gibson et al., 2006ab, 2011].

CONCLUSION

The results from experimental studies of current field characteristics in the Hawaiian (USA) and Gelendzhik (Black Sea, Russia) shelf areas and mathematical modelling data show that detected extreme surges of current velocities near submerged wastewater discharges registered by acoustic profilers are most probably related with vortex formation in convective plumes of low-salinity wastewaters. In both cases in Hawaiian shelf and Gelendzhik shelf areas narrow anticyclonic vortices ("vortex columns") were observed with orbital velocities of tens of cm/s and diameters considerably less than the distance between the instrument beams. Formation

[†] Turbulence is defined as an eddy-like state of fluid motion where the inertial vortex forces $v \times \omega$ of the eddies are larger than any other forces that tend to damp the eddies out. By this definition turbulence always cascades from small scales to large, and then fossilizes. Fossil turbulence is a perturbation produced by turbulence in any hydrophysical field that persists after the fluid is not longer turbulent at the scale of the perturbation.

of such “vortex columns” near submerged wastewater discharges might takes place regardless of whether the density stratification exists near the discharge or not. Future studies of different outfalls, and other oceanic studies of heat, mass, species and information vertical transport, should include determination of hydrodynamic phase diagrams in the receiving waters to better characterize the relevant fossil turbulence and fossil turbulence wave parameters.

REFERENCES

1.ADCP Coordinate Transformation: Formulas and Calculations // TELEDYNE RD INSTRUMENTS, P/N 951-6079-00 (January 2008*).*

2. *Bondur V.G.* Complex Satellite Monitoring of Coastal Water Areas 31st International Symposium on Remote Sensing of Environment. ISRSE, 2006, 7 p.

3.*Bondur V.G.* Satellite monitoring and mathematical modelling of deep runoff turbulent jets in coastal water areas // in book Waste Water - Evaluation and Management, ISBN 978-953-307-233-3, InTech, Croatia, 2011, pp. 155-180 http:// www.intechopen.com/articles/show/title/satellite-monitoring-and-mathematical-modelling-of-deep-runoff-turbulent-jets-in-coastal-water-areas

4.*Bondur. V., Tsidilina M.* “Features of Formation of Remote Sensing and Sea truth Databases for The Monitoring of Anthropogenic Impact on Ecosystems of Coastal Water Areas.” 31st International Symposium on Remote Sensing of Environment. ISRSE, 2006. pp. 192-195.

5.*Bondur V.G., Grebenyuk Y.V., Sabinin K.D.* Peculiarities of Internal Tidal Wave Generation near Oahu Osland (Hawaii). // Oceanology. 2009. V. 49 №3 pp. 299–309 (a)

6.*Bondur V.G., Grebenyuk Y.V., Sabinin K.D.* Peculiar Discontinuities in Small-Scale Currents at the Shelf in the Area of Natural Convection Impact. Doklady Earth Sciences. 2009 V. 429 №1 pp. 1389–1393 (b)

7.*Bondur V., Grebenyuk Yu., Sabinin K.* Thin vortexes in the current field of Mamala Bight (Hawaii) // Proc. of Int.Conf. Fluxes and structures in fluids, Moscow, June, 2009 (c).

8.*Bondur V.G., Grebenyuk Y.V., Muyakshin S.I., Sabinin K.D*. Fine Vortex Columns on the Shelf in the Area of Bottom Convection Influence. Izvestiya. Atmospheric and Oceanic Physics. 2011. V. 47 №2 pp. 233–240.

9.*Bondur V.G., Grebenyuk Yu.V., Tsidilina M.N., Filatov N.N., Zdorovennov R.E., Petrov M.P., Dolotov Yu.S.* Studies of hydrophysical processes during monitoring of the anthropogenic impact on coastal basins using the example of Mamala bay of Oahu island in Hawaii // Oceanology. 2007. V. 47 6 pp. 769-787

10. *Gibson, C. H.,* Internal waves, fossil turbulence, and composite ocean microstructure spectra, J. Fluid Mech., 1986, 168, 89-117.

11. *Gibson C.H., V.G. Bondur, R.N. Keeler, P.T. Leung*. Remote Sensing of Submerged Oceanic Turbulence and Fossil Turbulence, International Journal of Dynamics of Fluids, ISSN 0973-1784 Vol. 2, No. 2 , 2006a, 111-135; Journal of Cosmology, Vol. 21, pp 9199-9241.

12. *Gibson C.H., V.G. Bondur, R.N. Keeler, P.T. Leung.* Energetics of the Beamed Zombie Turbulence Maser Action Mechanism for Remote Detection of Submerged Oceanic Turbulence, Journal of Applied Fluid Mechanics, ISSN 1735-3645 Vol. 1, No. 1, 11-42, 2006b, 111-135; Journal of Cosmology, 2011, Vol. 17, pp 7751-7787.

13. *Gibson, C.H., Bondur, V.G., Keeler, R.N., Leung, P.T., Prandke, H., Vithanage, D.* 2007. Submerged turbulence detection with optical satellites, Proc. of SPIE, Coastal Remote Sensing, Aug. 26-27, edited by R. J. Frouin, Z. Lee, Vol. 6680, 6680X1-8. doi: 10.1117/12.732257. (b)

14. *Gibson C.H., Keeler R.N., Bondur V.G.* Vertical stratified turbulent transport mechanism indicated by remote sensing. Proceedings of SPIE, Coastal Remote Sensing. SPIE Newsroom, 2007. Vol. 6680 26-27 Aug. 2007 (a)

15. *Keeler R., Bondur V., Vithanage D*. Sea truth measurements for remote sensing of littoral water // Sea Technology, April, 2004, p. 53-58.

16. *Keeler R., Bondur V., Gibson C.* Optical satellite imagery detection of internal wave effects from a submerged turbulent outfall in the stratified ocean // Geophysical Research Letters, Vol. 32, L12610, doi: 10.1029/2005GL022390, 2005

17. *Konyaev K.B., Sabinin K.D.* Waves inside the Ocean, Gidrometeoizdat, St. Petersburg, 1992 [in Russian].

18. *Leung, P.T,* Coastal Microstructure: From Active Overturn to Fossil Turbulence, TAMU PhD Dissertation, Journal of Cosmology, 2011, Volume 17, pp 7612-7750.

19. *Wood I.R, Bell R.G, Wilkinson D.L.* Ocean disposal of wastewater. World Scientific. 1993. P.425.

20. *Zatsepin A.,V. Kremenetskiy, A.Korzh, A. Ostrovskii.* Submesoscale eddies at the narrow shelf: observations at the Black Sea // Proceed. 2nd Int. Conference "Dynamics of coastal zone of non-tidal seas". Kaliningrad. Terra Baltica. 2010. P.305-310.